The Preparation and Crystal Structure of the 3:1 Adduct of Antimony Trifluoride and Antimony Pentafluoride containing the $(Sb_3F_8^+)_\infty$ Cation †

W. A. Shantha Nandana, Jack Passmore,* D. C. Neil Swindells, Peter Taylor, and Peter S. White *
Department of Chemistry, University of New Brunswick, Fredericton, New Brunswick E3B 6E2, Canada
John E. Vekris
Department of Chemistry, McMaster University, Hamilton, Ontario L8S 4MI, Canada

Antimony pentafluoride and $SbF_3 \cdot SbF_5$ are reduced by an excess of phosphorus trifluoride, in liquid arsenic trifluoride to form $(SbF_3)_3SbF_5$ together with possibly small amounts of antimony trifluoride. Antimony pentafluoride is similarly reduced by an excess of elemental iodine to $(SbF_3)_3SbF_5$ but with larger amounts of antimony trifluoride. A single crystal *X*-ray diffraction study of $(SbF_3)_3SbF_5$ shows that it is monoclinic, space group $P2_1/m$, with cell dimensions $a = 10.895(3)$, $b = 10.941(3)$, $c = 4.772(1)$ Å, $\beta = 96.66(3)°$, and $Z = 2$. The structure was refined to a final *R* of 0.039 for 1 694 reflections. The structure consists of discrete SbF_6^- anions and parallel strands of $(Sb_3F_8^+)_\infty$ which lie along the *b* axis. The polymeric strand can be considered to be composed of SbF_3 and $Sb_2F_5^+$ units joined by antimony–fluorine bridges [2.270(5), 2.414(5) Å]. The vibrational spectrum of $(SbF_3)_3SbF_5$ is reported.

Antimony pentafluoride is a very strong Lewis acid,[1-6] and it is therefore not surprising that it forms adducts with antimony trifluoride. This class of antimony binary fluorides were first investigated by Ruff and Plato[7] in 1904. They reported that a series of adducts were formed between antimony pentafluoride and antimony trifluoride of composition $(SbF_3)_nSbF_5$ ($n = 2$, 5, and possibly 3 and 4). More recently $SbF_3 \cdot SbF_5$,[8] $(SbF_3)_6(SbF_5)_5$,[9] and $(SbF_3)_2SbF_5$[10] have been unambiguously characterised by single crystal *X*-ray diffraction studies.

One route to antimony fluorides of this type is the reduction of antimony pentafluoride with non-metals. For example, an excess of antimony pentafluoride and iodine react quantitatively according[11] to equation (1).

$$2I_2 + 6SbF_5 \xrightarrow[r.t.]{AsF_3} 2[I_2^+][Sb_2F_{11}^-] + SbF_3 \cdot SbF_5 \quad (1)$$

A similar reaction but with an excess of iodine led to $[I_5^+][SbF_6^-]$[12] and a reduced antimony fluoride whose Raman spectrum was different from those of other antimony fluorides.[13-15] We determined the nature of this new species, as it was of interest in its own right as a new binary fluoride of antimony, and also in order to understand, and more effectively design, reactions between antimony pentafluoride and an excess of non-metals that lead to novel antimony hexafluoride salts of homoatomic cations[12] and related species ($[S_7I^+][SbF_6^-]$).[16,17]

Experimental

Reagents and Apparatus.—Apparatus, chemicals, and techniques, unless otherwise specified, are as described in refs. 18—21. *X*-Ray powder diffraction photographs were obtained using a Philips Debye-Scherrer powder camera with Straumanis loading and nickel-filtered Cu-K_α radiation.[20] Raman spectra were obtained using a Spex Ramalab spectrometer and a Spectra Physics 2W krypton-argon, or 2W argon-ion lasers, both with the 5 145 Å line. Solids were manipulated in a Vacuum Atmospheres dri-lab fitted with a dri-train (HE-493). The adduct $SbF_3 \cdot SbF_5$ was prepared according to ref. 22. Reactions were carried out in well dried Pyrex vessels equipped with Teflon stemmed J. Young glass valves, and those using iodine in two bulbed (each 20 cm³) vessels incorporating a coarse sintered glass frit.

Preparation of $(SbF_3)_3SbF_5$.—(*a*) Phosphorus trifluoride was condensed into a clear solution of antimony pentafluoride in arsenic trifluoride and after *ca.* 3 h at room temperature (r.t.) a white precipitate was formed. Gaseous products were monitored daily by i.r. spectroscopy and each time the sample was returned to the reaction vessel. The reaction was judged complete when the phosphorus pentafluoride concentration was approximately constant. The volatiles [AsF_3, PF_5, PF_3, and small amounts of $P(O)F_3$] were removed leaving a colourless crystalline solid product. Translucent single crystals were formed in all reactions, and in some cases the product appeared to consist of homogeneous crystals of $(SbF_3)_3SbF_5$. Reaction data are given in Table 1.

Raman spectra of the crystal from which *X*-ray diffraction data were collected were obtained in various directions and the spectra were found to be dependent on orientation (Table 2).‡ Another large single crystal was found to be identical to the first by precession photography and Raman spectroscopy. This crystal was crushed and the Raman spectrum of the powder obtained ‡ (Table 2). The Raman spectra of other large crystals were obtained to establish their identity and they were ground into a powder from which an *X*-ray powder diffraction photograph and i.r. spectrum between AgCl plates were obtained.‡ The intensities and positions of the lines of the powder photograph were accounted for on the basis of the $(SbF_3)_3SbF_5$ single-crystal data. This powder photograph was then used as a standard against which other $(SbF_3)_3SbF_5$ samples were judged. *X*-Ray powder diffraction photographs of the bulk product of these reactions were identical to that of $(SbF_3)_3SbF_5$ except for possibly very weak lines attributable to antimony trifluoride. Raman spectra of the bulk material were identical to that of $(SbF_3)_3SbF_5$. The melting point of $(SbF_3)_3SbF_5$ is 190—192 °C as determined with the sample in a sealed melting point tube. Melting points (at *ca.* 200 °C) of various compounds determined in this manner (in melting point tubes) gave values *ca.* 4.5 °C lower than when determined conventionally. *X*-Ray powder photographs of mixtures of $(SbF_3)_3SbF_5$ and SbF_3 were obtained at various relative concentrations and it was found difficult to detect

---

† *Supplementary data available* (No. SUP 23504, 22 pp.): structure factors, thermal parameters, Raman and infrared spectra of $(SbF_3)_3SbF_5$. See Notices to Authors No. 7, *J. Chem. Soc., Dalton Trans.*, 1981, Index issue.

Non-S.I. unit employed: 1 atm = 101 325 N m⁻².

‡ Copies of the actual spectra are deposited (see SUP 23504).

Table 1. Data for various $(SbF_3)_3SbF_5$ preparations

	Reactants									
	SbF_5		PF_3							
Expt.	g	mmol	g	mmol	Solvent AsF_3/mmol	t/d	Weight of reduced antimony fluoride [a]/g	SbF_x [b]		
1	2.796	12.90	1.199	13.63	72.4	18	2.448 [c]	3.58		
2	3.422	15.79	1.100	12.50	85.6	20	3.029 [c]	3.69		
3	4.569	21.08	1.815	20.63	54.5	21	4.015 [c]	3.62		
4	3.810	17.58	*d*		72.4	20	3.346 [c]	3.61		
									$[I_5^+][SbF_6^-]$ [f]	
	SbF_5		I_2						g	mmol
5	4.375	20.19	13.078	51.53	84.1	4	1.402 [e]	3.43	10.257	11.79
6	9.350	43.13	32.690	128.80	67.0	21	2.960 [e]	3.37	22.260	25.99
	$(SbF_3)_3SbF_5$		PF_3							
7 [g]	2.230	3.00	0.410 0.780	4.70 8.87	57.60	5 8	2.210			
	$SbF_3{\cdot}SbF_5$		PF_3							
8 [h]	2.530	6.40	7.30	83.0 (50 atm)	87.3	7				
	$(SbF_5)_3SbF_5$ [i]		PF_3							
9 [j]	1.130	1.50	4.78	54.3 (50 atm)		14				

[a] Identified as $(SbF_3)_3SbF_5$ by Raman spectroscopy and *X*-ray powder photography. [b] Value of x calculated from appropriate antimony fluoride reactant and product weights. [c] Possibly contains a trace of SbF_3 as detected by *X*-ray powder photography. [d] Four aliquots of 1 g each (5 d residency time) added after previous aliquot was removed. [e] SbF_3 also a product and clearly detected by *X*-ray powder diffraction photography. [f] See ref. 12. [g] The reaction was carried out in a Teflon vessel. After reacting with the first aliquot of PF_3 for 5 d, the volatiles were removed and the second aliquot of PF_3 was added. No PF_5 or $P(O)F_3$ was observed after reaction with each aliquot. Raman spectrum and powder photographs of reactant and product were identical. [h] The reaction was carried out in a 45 cm³ Monel Parr bomb at r.t. Product identified as $(SbF_3)_3SbF_5$ by Raman spectroscopy. [i] At 250 °C. [j] The reaction was carried out in a 45 cm³ Monel Parr bomb. Product identified as SbF_3 by Raman spectroscopy and *X*-ray powder photography.

Table 2. Vibrational spectrum [a] of $(SbF_3)_3SbF_5$

Powder		Raman (single crystal) [b]		$Li(SbF_6)$ [c]		Tentative assignments
I.r.[d]	Raman [b]	Orientation A [e]	Orientation B	I.r.	Raman	
	264 (sh)	261 (0.5)				
	278 (1.3)	278 (2.1)				$(Sb_3F_8^+)_\infty$?
	285 (sh) (0.3)		285 (0.3)			
	291 (1.0)		292 (0.9)		294 (4.4)	SbF_6^-, ν_5
	294 (sh) (0.5)	294 (1.5)				
	304 (sh)	303 (sh)				
	427vbr [f] (3.0)	427br (9.8)				
505w, br						$(Sb_3F_8^+)_\infty$
540w	533 (2.3)		533 (4.9)			
	555 (sh) (1.6)	555 (2.2)	555 (sh)		558 (2.1)	SbF_6^-, ν_2
565w						?
	568 (4.7)	568 (3.2)	568 (6.8)			$(Sb_3F_8^+)_\infty$
	580 (8.7)	581 (2.8)	581 (10.0)			$(Sb_3F_8^+)_\infty$
	616 (0.4)	614 (0.5)	614 (0.4)			*g*
624m						*g*
	640 (0.4)	641 (sh) (0.3)	638 (sh) (0.4)			*g*
653s	653 (10.0)	653 (10.0)	652 (4.1)	669s	668 (10)	SbF_6^-, ν_1, ν_3
	663 (sh) (0.2)	663 (sh) (0.2)	662 (sh) (0.2)			*g*
685m						*g*

[a] In cm⁻¹. Copies of the actual spectra are deposited (see SUP 23504). [b] Intensities in parentheses; sh = shoulder. [c] G. M. Begun and A. C. Rutenberg, *Inorg. Chem.*, 1967, **6**, 2216. $Li(SbF_6)$ peak at 350 cm⁻¹ not included in the Table. [d] Powder between KBr plates. The spectrum using AgCl plates was the same. [e] Orientation of A approximately 90° to that of B. Third orientation, approximately 90° to A and B gave spectra similar to B. [f] Exact location of centre of broad band uncertain. [g] Probably SbF_6^- arising from slight distortion from octahedral symmetry.

small amounts (less than 10 mol per cent) of SbF_3 in $(SbF_3)_3SbF_5$.

(*b*) Antimony pentafluoride was reacted with an excess of iodine in arsenic trifluoride as described in ref. 12. Data are given in Table 1.

X-Ray Crystal Structure of $(SbF_3)_3SbF_5$.—*Crystal data.* $(SbF_3)_3SbF_5$, Monoclinic, $M = 753.0$, $a = 10.895(3)$, $b = 10.941(3)$, $c = 4.772(1)$ Å, $\beta = 96.66(3)°$, $U = 565.0(5)$ Å^3, $Z = 2$, $D_c = 4.43$ g cm^{-3}, $F(000) = 660$, space group $P2_1/m$, Mo-K_α radiation, $\lambda = 0.710\,69$ Å, $\mu = 9.70$ mm^{-1}, crystal size 0.63 × 0.44 × 0.22 mm.

A suitable single crystal was mounted under nitrogen in a rigorously dried Pyrex capillary. A preliminary photographic study showed the crystal to be monoclinic, space group $P2_1/m$ or $P2_1$, and yielded initial cell parameters. Accurate cell parameters were obtained using a least-squares fit of cell dimensions and an orientation matrix to the diffractometer settings for 11 well centred reflections ($44 \leqslant 2\theta \leqslant 46°$).

Intensities were collected on a Picker FACS-I four-circle diffractometer using graphite crystal monochromated Mo-K_α radiation. An ω—2θ scan with a base width of 2° (2θ) corrected for dispersion of the K_α doublet, and a scan rate of 1° min^{-1}, were employed. Background intensity was estimated from 10-s counts made at each end of the scan. The intensities of three standard reflections measured every 100 reflections did not vary significantly during data collection.

A total of 1 735 independent reflections were measured for $2\theta \leqslant 60°$. Of these, 1 694 (97.6%) were classed as observed, being greater than $3\sigma(I)$ where $\sigma(I)$ is estimated from counter statistics, and included in the subsequent refinement.

Structure determination and refinement. Data reduction and structure refinement utilized the *X*-RAY 76 program package.[23] Atomic scattering factors for the neutral atoms were taken from Cromer and Mann,[24] and the antimony scattering factors were corrected for anomalous dispersion. The data were corrected for absorption; transmission factors were in the range 0.030—0.148. Initial positional parameters were determined using the MULTAN system of direct methods programs,[25] in the space group $P2_1/m$, which gave the positions of the three antimony atoms. A subsequent Fourier synthesis determined the positions of the fluorine atoms. The structure was refined in space group $P2_1/m$ by full-matrix least-squares techniques in which the function minimised was $\Sigma w(|F_o| - |F_c|)^2$. Weights of the form $w = 1/\sigma(F)^2$, where $\sigma(F)$ is directly derived from $\sigma(I)$, were modified by a series of the form $w' = 1/(a + b/w + cF_o)$ such that an analysis of $w(|F_o| - |F_c|)^2$ as a function of sin θ and F_o remained constant. With the thermal parameters of all atoms varied anisotropically and a dispersion correction applied, the refinement converged to $R = 0.039$, $R' = 0.047$ for the 1 694 reflections. Average shift-to-error for the final cycle was 0.043 with a maximum value of 0.175 associated with a fluorine atom. Final positional parameters are given in Table 3. A ΔF synthesis at this point showed a maximum electron density of 2.12 e Å^{-3} at −0.1489, 0.2500, 0.8504, *i.e.* associated with Sb(3), indicating no misplaced or uncounted atoms. An attempt to refine the structure in space group $P2_1$ did not result in an improvement of the *R* factor indicating that $P2_1/m$ was the correct choice.

Results and Discussion

Preparation of $(SbF_3)_3SbF_5$.—Crystalline $(SbF_3)_3SbF_5$ was prepared essentially quantitatively (see Table 1) by the reduction of antimony pentafluoride in arsenic trifluoride with phosphorus trifluoride according to equation (2).

Table 3. Final atomic positional parameters (fractional × 10^4) with estimated standard deviations in parentheses

Atom	*x*	*y*	*z*
Sb(1)	5 244(1)	2 500	4 330(1)
Sb(2)	2 315(1)	4 383(1)	8 017(1)
Sb(3)	−795(1)	2 500	8 915(1)
F(1)	2 210(6)	2 500	6 751(13)
F(2)	3 800(7)	2 500	1 733(15)
F(3)	2 118(5)	4 817(5)	4 155(10)
F(4)	6 654(7)	2 500	6 910(17)
F(5)	5 921(5)	1 276(5)	2 247(11)
F(6)	−1 553(5)	1 280(4)	11 341(12)
F(7)	533(4)	4 137(5)	7 706(13)
F(8)	557(7)	2 500	11 726(19)
F(9)	4 535(5)	3 708(5)	6 449(11)

$$4SbF_5 + 3PF_3 \xrightarrow[\text{r.t.}]{AsF_3} (SbF_3)_3SbF_5 + 3PF_5 \qquad (2)$$

Arsenic trifluoride and antimony pentafluoride have been shown[26] to form $AsF_3{\cdot}SbF_5$ which with excess arsenic trifluoride may form the species $(AsF_3)_xSbF_5$ where $x > 1$. Reduction presumably proceeds through various $(SbF_3)_x(SbF_5)_y$ adducts, one of which $SbF_3{\cdot}SbF_5$[8] was separately reacted (Table 1) with an excess of phosphorus trifluoride under similar conditions yielding $(SbF_3)_3SbF_5$. Antimony trifluoride was not detected in good quality Raman spectra of these products. *X*-Ray powder photographs showed the presence of $(SbF_3)_3SbF_5$ and possibly small amounts of antimony trifluoride. Interestingly, $(SbF_3)_3SbF_5$ did not appear to be further reduced by very large excesses of phosphorus trifluoride at room temperature. Antimony trifluoride was formed on heating $(SbF_3)_3SbF_5$ and PF_3 in a solid-gas reaction.

This study was initiated by the observation that excess iodine and antimony pentafluoride in arsenic trifluoride solution gave $[I_5^+][SbF_6^-]$[12] and a reduced antimony fluoride whose chemical analysis was consistent with that of antimony trifluoride, but with a Raman spectrum that was not.[14,15] This reaction was repeated and reaction data (Table 1) were those expected for equation (3), excepting that weights of $(SbF_3)_3SbF_5$ were slightly low. Raman spectra of the insoluble antimony fluoride were not of good quality but were essentially identical to that of $(SbF_3)_3SbF_5$ (Table 2) except in one case in which weak peaks attributable to antimony trifluoride were observed. However, *X*-ray powder diffraction photographs clearly showed the product to be a mixture of $(SbF_3)_3SbF_5$ and lesser amounts of antimony trifluoride. The relative amount of antimony trifluoride, as judged by *X*-ray powder photography, varied from reaction to reaction and did not appear to be related to the extent of the excess of iodine, or the reaction time. The problem could also be further complicated if the crystallinity (and therefore extent of diffraction of *X*-rays, and Raman scattering) varied from sample to sample. The original sample of antimony fluoride formed by reduction of antimony pentafluoride and excess iodine[12] which analysed as SbF_3 was likely a mixture of $(SbF_3)_3SbF_5$ (clearly identified by Raman spectroscopy) and SbF_3 (not readily identified in these samples by Raman spectroscopy). Thus chemical analysis data would be very similar to that expected for antimony trifluoride. We also add that elemental analyses obtained for samples of this sort, from first class

$$15I_2 + 10SbF_5 \xrightarrow[\text{r.t.}]{AsF_3} 6[I_5^+][SbF_6^-] + (SbF_3)_3SbF_5 \qquad (3)$$

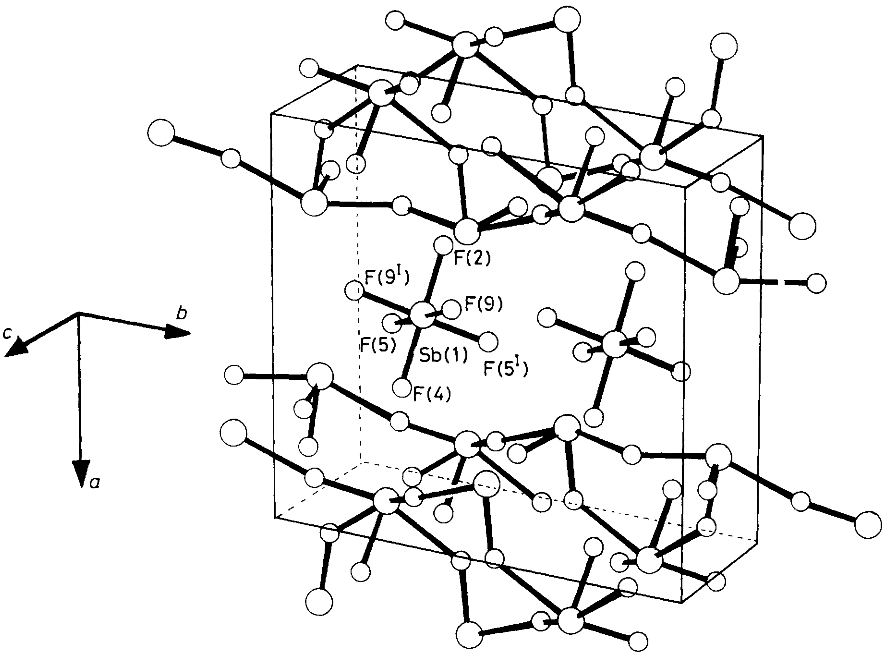

Figure 1. Crystal packing of $(SbF_3)_3SbF_5$

commercial analytical services, were not infrequently inconsistent.

We have also unambiguously identified $(SbF_3)_3SbF_5$ as a product of the reaction of antimony pentafluoride with an excess of iodine and sulphur in sulphur dioxide solution leading to $[S_7I^+][SbF_6^-]$ [16] and in two other related reactions.[17,27] However antimony trifluoride has been reported as the only product of similar reactions [28,29] of antimony pentafluoride with excess of other reducing reagents.

The results taken as a whole suggest the absence of definite adducts of a composition intermediate between that of antimony trifluoride and $(SbF_3)_3SbF_5$ in systems of this sort. The adducts $(SbF_3)_nSbF_5$ (n = 2, 5, and possibly 3 and 4) reported by Ruff and Plato [7] were prepared by distillation at high temperatures of mixtures of antimony tri- and pentafluorides; that is under very different conditions to those encountered in this work. Our $(SbF_3)_3SbF_5$ may or may not be the adduct $(SbF_3)_nSbF_5$ (n = 3) reported by Ruff and Plato.[7]

Structure of $(SbF_3)_3SbF_5$.—The crystal packing of $(SbF_3)_3SbF_5$ is shown in Figure 1, the corresponding bond distances are given in Table 4, and bond angles in Table 5.

The structure is made up of discrete SbF_6^- anions and parallel strands of $(Sb_3F_8^+)_\infty$ that lie along the b axis (Figure 2). Interstrand distances are essentially greater or equal to the sum of the van der Waals radii of antimony and fluorine (3.50 Å) except for one contact [Sb(2)–F(3^{II})] at 3.000(5) Å and another [Sb(2)–F(8)] at 3.439(7) Å. The SbF_6^- anion has a slightly distorted octahedral structure with a mean Sb^V–F distance of 1.87(1) Å, similar to that found in other hexafluoroantimonate anions.[30] The vibrational spectrum of $(SbF_3)_3SbF_5$ is consistent with the presence of a slightly distorted octahedral SbF_6^- (see Table 2). Fluorine atoms in the SbF_6^- cation bridge to antimony atoms of $(Sb_3F_8^+)_\infty$ with contacts in the range 2.716—3.056 Å. The structure of the strand is reminiscent of strands of $(TeF_3^+)(TeF_4)_2$ in $Os(O)(OTeF_5)_4(F^-)(TeF_3^+)(TeF_4)_2$.[31]

Table 4. Bond lengths (Å) (⩾3.50 Å) with estimated standard deviations in parentheses

Sb(1)–F(4)	1.853(7)
Sb(1)–F(5)	1.870(5)
Sb(1)–F(9)	1.883(5)
Sb(1)–F(2)	1.887(7)
Sb(2)–F(3)	1.890(5)
Sb(2)–F(7)	1.949(5)
Sb(2)–F(1)	2.146(2)
Sb(2)–F(6)	2.270(5)
Sb(2)–F(9)	2.716(5)
Sb(2)–F(5)	2.838(5)
Sb(2)–F(3^{II})*	3.000(5)
Sb(2)–F(2)	3.056(5)
Sb(2)–F(8)	3.439(7)
Sb(3)–F(8)	1.874(8)
Sb(3)–F(6)	2.006(5)
Sb(3)–F(7)	2.414(5)
Sb(3)–F(4)	2.833(7)

* Roman numeral superscript refers to position x, y, $1 + z$.

Within the polymeric cation separate SbF_3 and $Sb_2F_5^+$ units can be distinguished if only the shorter (⩽2.15 Å) bonds are considered. The SbF_3 and $Sb_2F_5^+$ are joined by antimony fluorine bridging bonds [Sb(3)–F(6), 2.006(5); Sb(2)–F(6) at 2.270(5) Å] to form two approximately parallel chains within the cation. These chains are joined by the weakest bridging bond [Sb(3)–F(7) at 2.414(5) Å] within the polymeric strand.

The structure of the SbF_3 unit within the cation is similar to that of antimony trifluoride [32] itself (Figure 3). The Sb(3)–F(8) bond is shorter than Sb(3)–F(6) reflecting the strong bridge formed by F(6) to Sb(2) of $Sb_2F_5^+$ to give $Sb_3F_8^+$. The angles in $Sb(3)F_3$, and around Sb(2) as well as those related bond angles in antimony trifluoride,[32] $SbF_3 \cdot SbF_5$,[8] and $(SbF_3)_5(SbF_3)_6$,[9] are less than 90° consistent with the presence of sterically active lone pairs.[33] In valence shell electron pair repulsion (v.s.e.p.r.) theory terms, the overall geometry of Sb(3) within the $(Sb_3F_8^+)_\infty$ cation is square pyramidal

Table 5. Bond angles (°) with estimated standard deviations in parentheses

(*a*) Sb–F $\leqslant$ 2.5 Å			
F(2)–Sb(1)–F(4)	179.4(3)	F(3)–Sb(2)–F(6$^{\mathrm{IV}}$)	84.3(2)
F(2)–Sb(1)–F(5)	90.1(2)	F(3)–Sb(2)–F(7)	87.8(2)
F(2)–Sb(1)–F(9)	89.4(2)	F(6$^{\mathrm{IV}}$)–Sb(2)–F(7)	76.1(2)
F(4)–Sb(1)–F(5)	90.3(2)	F(6)–Sb(3)–F(7)	158.4(2)
F(4)–Sb(1)–F(9)	90.2(2)	F(6)–Sb(3)–F(8)	85.9(2)
F(5)–Sb(1)–F(9)	178.7(3)	F(6)–Sb(3)–F(6$^{\mathrm{I}}$)	83.4(2)
F(5)–Sb(1)–F(5$^{\mathrm{I}}$)	91.5(2)	F(6)–Sb(3)–F(7$^{\mathrm{I}}$)	86.7(2)
F(5)–Sb(1)–F(9$^{\mathrm{I}}$)	89.7(2)	F(7)–Sb(3)–F(8)	74.2(2)
F(9)–Sb(1)–F(9$^{\mathrm{I}}$)	89.1(2)	F(7)–Sb(3)–F(7$^{\mathrm{I}}$)	95.8(2)
F(1)–Sb(2)–F(3)	88.3(3)	Sb(2)–F(1)–Sb(2$^{\mathrm{I}}$)	147.4(3)
F(1)–Sb(2)–F(7)	80.0(2)	Sb(3)–F(6)–Sb(2$^{\mathrm{VI}}$)	150.2(3)
F(1)–Sb(2)–F(6$^{\mathrm{IV}}$)	155.2(2)	Sb(2)–F(7)–Sb(3)	134.7(3)
(*b*) 2.5 < Sb–F $\leqslant$ 3.5 Å			
F(1)–Sb(2)–F(8)	63.6(2)	F(9)–Sb(2)–F(2$^{\mathrm{II}}$)	63.1(2)
F(1)–Sb(2)–F(9)	71.4(2)	F(9)–Sb(2)–F(3$^{\mathrm{II}}$)	118.6(2)
F(1)–Sb(2)–F(2$^{\mathrm{II}}$)	61.6(2)	F(9)–Sb(2)–F(5$^{\mathrm{III}}$)	63.7(2)
F(1)–Sb(2)–F(3$^{\mathrm{II}}$)	114.8(2)	F(9)–Sb(2)–F(6$^{\mathrm{IV}}$)	129.6(2)
F(1)–Sb(2)–F(5$^{\mathrm{III}}$)	134.6(2)	F(2$^{\mathrm{II}}$)–Sb(2)–F(3$^{\mathrm{II}}$)	68.5(2)
F(3)–Sb(2)–F(8)	130.2(2)	F(2$^{\mathrm{II}}$)–Sb(2)–F(5$^{\mathrm{III}}$)	101.6(1)
F(3)–Sb(2)–F(9)	78.7(2)	F(2$^{\mathrm{II}}$)–Sb(2)–F(6$^{\mathrm{IV}}$)	135.7(2)
F(3)–Sb(2)–F(2$^{\mathrm{II}}$)	136.7(2)	F(3$^{\mathrm{II}}$)–Sb(2)–F(5$^{\mathrm{III}}$)	93.0(1)
F(3)–Sb(2)–F(3$^{\mathrm{II}}$)	154.0(2)	F(3$^{\mathrm{II}}$)–Sb(2)–F(6$^{\mathrm{IV}}$)	69.8(2)
F(3)–Sb(2)–F(5$^{\mathrm{III}}$)	77.0(2)	F(5$^{\mathrm{III}}$)–Sb(2)–F(6$^{\mathrm{IV}}$)	66.3(2)
F(7)–Sb(2)–F(8)	49.2(2)	F(4$^{\mathrm{V}}$)–Sb(3)–F(6)	75.0(2)
F(7)–Sb(2)–F(9)	148.5(2)	F(4$^{\mathrm{V}}$)–Sb(3)–F(7)	120.7(1)
F(7)–Sb(2)–F(2$^{\mathrm{II}}$)	114.0(2)	F(4$^{\mathrm{V}}$)–Sb(3)–F(8)	154.3(3)
F(7)–Sb(2)–F(3$^{\mathrm{II}}$)	85.0(2)	Sb(2$^{\mathrm{VII}}$)–F(2)–Sb(1)	136.6(1)
F(7)–Sb(2)–F(5$^{\mathrm{III}}$)	140.5(2)	Sb(2$^{\mathrm{VII}}$)–F(2)–Sb(2$^{\mathrm{VIII}}$)	84.8(2)
F(8)–Sb(2)–F(9)	123.1(1)	Sb(2)–F(3)–Sb(2$^{\mathrm{VII}}$)	154.0(3)
F(8)–Sb(2)–F(2$^{\mathrm{II}}$)	65.6(2)	Sb(1)–F(4)–Sb(3$^{\mathrm{IX}}$)	158.3(4)
F(8)–Sb(2)–F(3$^{\mathrm{II}}$)	59.0(2)	Sb(1)–F(5)–Sb(2$^{\mathrm{X}}$)	149.0(2)
F(8)–Sb(2)–F(5$^{\mathrm{III}}$)	151.7(2)	Sb(2)–F(8)–Sb(3)	94.0(3)
F(8)–Sb(2)–F(6$^{\mathrm{IV}}$)	104.1(2)	Sb(2)–F(8)–Sb(2$^{\mathrm{I}}$)	73.6(2)
		Sb(1)–F(9)–Sb(2)	140.6(2)

Roman numeral superscripts refer to atoms in the positions: I $x, \frac{1}{2} - y, z$; II $x, y, 1 + z$; III $1 - x, \frac{1}{2} + y, 1 - z$; IV $-x, \frac{1}{2} + y, 2 - z$; V $-1 + x, y, z$; VI $-x, -\frac{1}{2} + y, 2 - z$; VII $x, y, -1 + z$; VIII $x, \frac{1}{2} - y, -1 + z$; IX $1 + x, y, z$; X $1 - x, -\frac{1}{2} + y, 1 - z$.

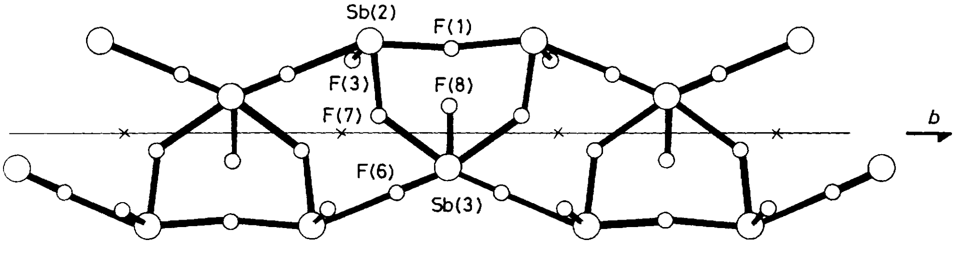

Figure 2. $(Sb_3F_8^+)_\infty$ strand

AXY_4E, with the shortest antimony–fluorine bond (X) *trans* to the lone pair (E) and the equatorial bonds bent back from the lone pair with Sb(3) above [0.395(1) Å] the plane containing the four equatorial fluorine atoms (Y_4) as defined in Figure 3. The complete co-ordination around Sb(3) [contacts $\leqslant$3.50 Å] within the whole structure is given by the inclusion of one weak contact [2.833(7) Å] with F(4) of the SbF_6^-, and can be described, like SbF_3 itself, as a monocapped octahedron AX_3Y_3E (see Figure 3). The geometry about Sb(3) is also similar to that of the antimony atoms in $K(SbF_4)$ [34] which also can be regarded as variously AX_3E, AXY_4E, and AX_3Y_3E as an increasing number of fluorine atoms are included in the co-ordination sphere of antimony. The bond angle variations and the deviation of the bond angles from those expected for the various regular geometries are consistent with the v.s.e.p.r. model with the lone pair in the position intermediate between that expected for an AX_3E (or AX_3Y_3E) and an AXY_4E configuration (see Figure 3).

The geometry of $Sb_2F_5^+$ in $(SbF_3)_3SbF_5$ is given in Figure 4(*i*) which is the same as that of the isoelectronic $(SF_2)_2N^+$ in $(SF_2)_2NAsF_6$.[35] The two Sb(2)F(3)F(7) units are related by a mirror plane that passes through the bridging F(1), and are therefore in an eclipsed position relative to the Sb(2)Sb(2) axis. The lone pairs on the two Sb(2) atoms are therefore also eclipsed. The configuration of the $Sb_2F_5^+$ in $(Se_4^{2+})(Sb_2F_4^{2+})$-$(Sb_2F_5^+)(SbF_6^-)_5$ [36] is intermediate between semi-eclipsed and *trans* [see Figure 4(*ii*)] although bond distances and angles are essentially the same as those of $Sb_2F_5^+$ in $(SbF_3)_3$-

Table 6. Distribution of bond valences [a] within $(\mathrm{SbF_3})_3\mathrm{SbF_5}$

					Total
	F(4) [b]	2 × F(5) [b]	2 × F(9) [b]	F(2) [b]	
$\mathrm{Sb^V}$(1)	0.91	2 × 0.85	2 × 0.81	0.80	5.03
	F(3)	F(7)	F(1)	F(6$^{\mathrm{IV}}$)	
$\mathrm{Sb^{III}}$(2)	0.79	0.70	0.49	0.40	
	F(9) [b]	F(5$^{\mathrm{III}}$) [b]	F(3$^{\mathrm{II}}$)	F(2$^{\mathrm{II}}$) [b]	
	0.21	0.18	0.14	0.13	
	F(8)				
	0.09				3.13
	F(8)	2 × F(6)	2 × F(7)	F(4) [b]	
$\mathrm{Sb^{III}}$(3)	0.81	2 × 0.63	2 × 0.32	0.18	
	2 × F(3)				
	2 × 0.08				3.05

[a] Bond valence(s) calculated according to equation (1) given in refs. 40 and 41: $s = [R/R_0]^{-n}$ (1), where for $\mathrm{Sb^{III}}$, $n = 3.7$, $R_0 = 1.772$ and for $\mathrm{Sb^V}$, $n = 7.3$, and $R_0 = 1.830$ (R = experimental bond distance, R_0 and n are constants for a given pair of atoms in given oxidation states. All bond valences $\geqslant 0.08$ are included. The sum of s values for all F atoms lies between 0.98 and 1.03). [b] These atoms are part of $\mathrm{SbF_6^-}$.

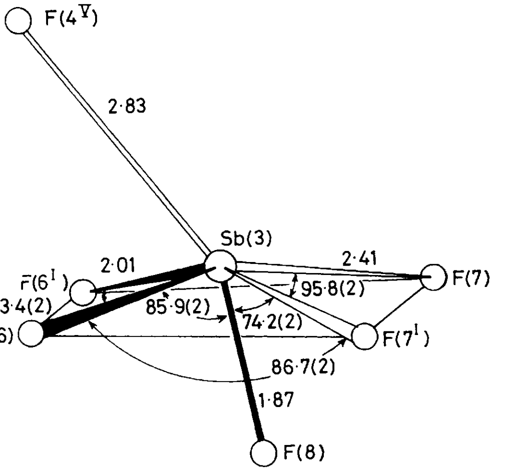

Figure 3. The structure of Sb(3)$\mathrm{F_3}$ within $(\mathrm{Sb_3F_8^+})_\infty$

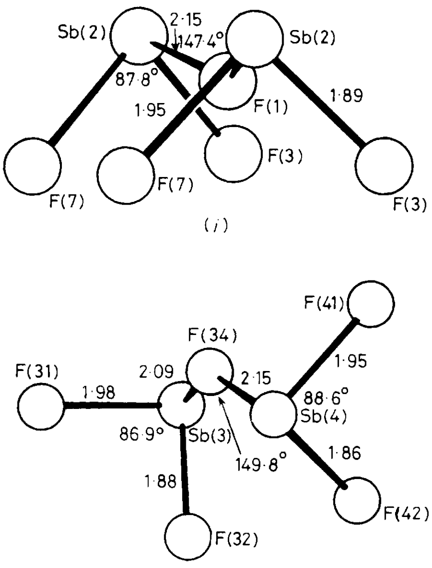

Figure 4. Geometries of $\mathrm{Sb_2F_5^+}$ in (*i*) $(\mathrm{SbF_3})_3\mathrm{SbF_5}$ and (*ii*) $(\mathrm{Se_4^{2+}})(\mathrm{Sb_2F_4^{2+}})(\mathrm{Sb_2F_5^+})(\mathrm{SbF_6^-})_5$ [36]

$\mathrm{SbF_5}$. The geometry of the isoelectronic $\mathrm{Sn_2F_5^-}$ [37] is similar to that of $\mathrm{Sb_2F_5^+}$ in $(\mathrm{Se_4^{2+}})(\mathrm{Sb_2F_4^{2+}})(\mathrm{Sb_2F_5^+})(\mathrm{SbF_6^-})_5$,[36] while $\mathrm{Sb_2F_3Cl_2^+}$ in $\mathrm{Sb_2F_4Cl_5}$ [38] has approximately a *gauche* configuration. Other $\mathrm{Sb_2F_5^+}$ geometries occur in $(\mathrm{SbF_3})_6(\mathrm{SbF_5})_5$ [9] and $(\mathrm{SbF_3})_5(\mathrm{SbF_5})_3$.[39] The energy differences between $\mathrm{Sb_2F_5^+}$ of differing geometries may be small, and the different configurations may arise from differences in secondary interactions.

The symmetrical bridging bond is longer than the others and the $\mathrm{Sb_2F_5^+}$ cation can be considered as comprising of two $\mathrm{SbF_2^+}$ units bridged through an $\mathrm{F^-}$ ion, or alternatively as arising from $\mathrm{SbF_3}$–$\mathrm{SbF_2^+}$, $\mathrm{SbF_2^+}$–$\mathrm{SbF_3}$ resonance structures. Thus, the co-ordination about Sb(2) can be regarded as $\mathrm{AX_3E}$. The co-ordination around Sb(2), including all intrastrand contacts, can be viewed as distorted $\mathrm{AX_2Y_2E}$, with the lone pair and other longer contacts reducing the F(1)–Sb(2)–F(6) angle [155.2(2)°] from 180°, and the F(3)–Sb(2)–F(7) angle [87.8(2)°] from 120°. The co-ordination around Sb(2), including all contacts less than 3.00 Å, is $\mathrm{AXY_5E}$ with the shortest bond Sb(2)–F(3) at 7.9° to the normal to the plane of the equatorial fluorine atoms illustrated in Figure 5. The five equatorial fluorine atoms are approximately planar, the sum of the angles being 357.5°. The Sb(2) atom is 0.257 Å above the equatorial plane as shown in Figure 5, and all five F(3)–Sb(2)–F(equatorial) angles are less than 90° consistent with the presence of a lone pair. Bond angles within the pentagon reflect relative bond–bond repulsions, *i.e.* the longer the adjacent bonds, the smaller is the angle. An $\mathrm{AXY_5E}$ geometry is observed for one of the antimony atoms in $\mathrm{SbF_3{\cdot}SbF_5}$ [8] and the antimony atoms of the $\mathrm{Sb_2F_4^{2+}}$ cations in $(\mathrm{Se_4^{2+}})(\mathrm{Sb_2F_4^{2+}})(\mathrm{Sb_2F_5^+})(\mathrm{SbF_6^-})_5$.[36] The complete co-ordination around Sb(2) is made by contacts at 3.056(5), 3.000(5), and another at 3.439(2) Å all of which approach Sb(2) from the side of the lone pair. The lone pair is in approximately the same place in all these various arrangements.

Brown [40,41] has proposed that 'the sum of the bond

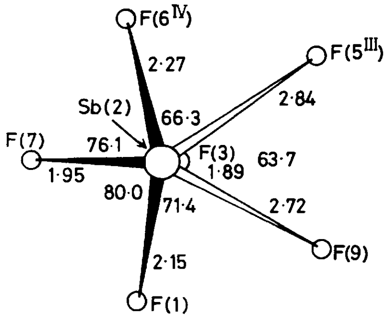

Figure 5. The co-ordination about Sb(2) including all contacts less than 3 Å. AX_2Y_2E co-ordination of Sb(2)F(3)F(7)F(1)F(6^{IV}) indicated by solid lines drawn between bonds. Addition of F(5^{III}) and F(9) atoms completes AXY_5E co-ordination around Sb(2)

valences around each atom must be equal to the atom valence' where the valence of an atom is the same as its formal oxidation state. Table 6 shows the values of the bond valence (proportional to bond strengths) assigned to each pair of interacting atoms in $(SbF_3)_3SbF_5$ using Brown's[40,41] empirical quantitative approach. It is seen that essentially three bond valences of each Sb^{III} atom are partitioned between all the strong and weak fluorine bonds to Sb^{III}, and similarly the one fluorine bond valence is shared between the bonds the fluorine atom makes to its antimony neighbours (generally two).

The structure is approximately closely packed with a volume per fluorine atom of 20.2 Å^3, but the packing is not as efficient as in SbF_5[42] with a volume per fluorine of 17.8 Å^3. However, it has been shown[43] that the lone pair on an Sb^{III} atom can be assumed to occupy a volume similar to that of a fluorine atom and then the volume per fluorine is 16.6 Å^3, that found for SbF_3[33] (16.75 Å^3) with the lone pair counted as a fluorine atom.

Acknowledgements

We wish to thank the Natural Sciences Engineering Research Council (Canada) for financial support.

References

1 M. Brownstein and R. J. Gillespie, *J. Am. Chem. Soc.*, 1970, **92**, 2718.
2 P. A. W. Dean and R. J. Gillespie, *J. Am. Chem. Soc.*, 1969, **91**, 7260.
3 G. S. H. Chen and J. Passmore, *J. Chem. Soc., Dalton Trans.*, 1979, 1251.
4 M. Cramer and L. C. Duncan, *Inorg. Chem.*, 1971, **10**, 647.
5 P. A. W. Dean, R. J. Gillespie, R. Hulme, and D. A. Humphreys, *J. Chem. Soc. A*, 1971, 341.
6 R. J. Gillespie, K. Ouchi, and G. P. Pez, *Inorg. Chem.*, 1969, **8**, 63.
7 O. Ruff and W. Plato, *Ber. Dtsch. Chem. Ges.*, 1904, **37**, 673.
8 R. J. Gillespie, D. R. Slim, and J. E. Vekris, *J. Chem. Soc., Dalton Trans.*, 1977, 971.
9 A. J. Edwards and D. R. Slim, *J. Chem. Soc., Chem. Commun.*, 1974, 178.
10 A. J. Edwards, personal communication.
11 J. Passmore, E. K. Richardson, and P. Taylor, *J. Chem. Soc., Dalton Trans.*, 1976, 1006.
12 J. Passmore, P. Taylor, T. K. Whidden, and P. S. White, *Can. J. Chem.*, 1979, **57**, 968.
13 T. Birchall, P. A. W. Dean, B. Della Valle, and R. J. Gillespie, *Can. J. Chem.*, 1973, **51**, 667.
14 C. J. Adams and A. J. Downs, *J. Chem. Soc. A*, 1971, 1534.
15 L. E. Alexander and I. R. Beattie, *J. Chem. Soc., Dalton Trans.*, 1972, 1745.
16 J. Passmore, G. Sutherland, P. Taylor, T. K. Whidden, and P. S. White, *Inorg. Chem.*, 1981, **20**, 3839 and refs. therein.
17 G. Sutherland, Ph.D. Thesis, University of New Brunswick, 1981.
18 G. S. H. Chen, J. Passmore, P. Taylor, and T. K. Whidden, *Inorg. Nucl. Chem. Lett.*, 1976, **12**, 943.
19 C. Lau and J. Passmore, *J. Chem. Soc., Dalton Trans.*, 1973, 2528.
20 C. D. Desjardins and J. Passmore, *J. Fluorine Chem.*, 1975, **6**, 379.
21 J. Passmore and P. Taylor, *J. Chem. Soc., Dalton Trans.*, 1976, 804.
22 J. Passmore, W. A. S. Nandana, E. K. Richardson, and P. Taylor, *J. Fluorine Chem.*, 1980, **15**, 435.
23 'The *X*-Ray System-Version of 1976,' ed. J. M. Stewart, Technical Report T.R. 446, Computer Science Centre, University of Maryland, U.S.A.
24 D. T. Cromer and J. B. Mann, *Acta Crystallogr., Sect. A*, 1968, **24**, 321.
25 G. Germain, P. Main, and M. M. Woolfson, *Acta Crystallogr. Sect. A*, 1971, **27**, 368.
26 A. J. Edwards and R. J. C. Sills, *J. Chem. Soc. A*, 1971, 942.
27 J. Passmore, G. Sutherland, and P. S. White, *Inorg. Chem.*, 1982, **21**, 2717.
28 C. G. Davies, R. J. Gillespie, P. R. Ireland, and J. M. Sowa, *Can. J. Chem.*, 1974, **52**, 2048.
29 R. J. Gillespie, J. P. Kent, J. F. Sawyer, D. R. Slim, and J. D. Tyrer, *Inorg. Chem.*, 1981, **20**, 3799.
30 A. F. Wells, 'Structural Inorganic Chemistry,' 4th edn., Oxford University Press, 1975 and refs. therein.
31 P. Huppmann, H. Labischinski, D. Lentz, H. Pritzkow, and K. Seppelt, *Z. Anorg. Allg. Chem.*, 1982, **487**, 7.
32 A. J. Edwards, *J. Chem. Soc. A*, 1970, 2751.
33 R. J. Gillespie, 'Molecular Geometry,' Van Nostrand Reinhold, London, 1972.
34 N. Habibi, B. Ducourant, B. Bonnet, and R. Fourcade, *J. Fluorine Chem.*, 1979, **13**, 34.
35 G. K. MacLean, J. Passmore, and P. S. White, *J. Chem. Soc., Dalton Trans*, submitted for publication.
36 G. Cardinal, R. J. Gillespie, J. F. Sawyer, and J. E. Vekris, *J. Chem. Soc., Dalton Trans.*, 1982, 765.
37 R. R. McDonald, A. C. Larson, and D. T. Cromer, *Acta Crystallogr.*, 1964, **17**, 1104.
38 U. Müller, *Z. Anorg. Allg. Chem.*, 1978, **447**, 171.
39 W. A. S. Nandana, J. Passmore, P. S. White, and C.-M. Wong, unpublished work.
40 I. D. Brown, *J. Solid State Chem.*, 1974, **11**, 214 and refs. therein.
41 I. D. Brown, *Chem. Soc. Rev.*, 1978, **7**, 359.
42 A. J. Edwards and P. Taylor, *Chem. Commun.*, 1971, 1376.
43 J. Galy, G. Meunier, S. Andersson, and A. Åström, *J. Solid State Chem.*, 1975, **13**, 142.

Received 12*th July* 1982; *Paper* 2/1183